

Master in Photonics

MASTER THESIS WORK

**Laser cooling of Ytterbium-171 in a Zeeman
Slower: Monte Carlo Analysis**

Jesús Romero González

Dr. Jordi Mompart Penina, (UAB)

Presented on date 19th July 2021

Registered at



Laser cooling of Ytterbium-171 in a Zeeman Slower: Monte Carlo Analysis

Jesús Romero González

Department of Physics, Universitat Autònoma de Barcelona, Cerdanyola del Vallès, E-08193, Spain

E-mail: jesus.romero.gonzalez@estudiantat.upc.edu

July 19, 2021

Abstract. In this Master Thesis we study the operation of a Zeeman slower to cool an atomic beam. In particular, we consider a beam formed by ^{171}Yb atoms interacting with a counter-propagating laser beam in such a way that, by means of the Doppler effect and the Stark shift of the atomic levels, the interaction is resonant at any point in the slower longitudinal axis. The transition used for the cooling of the ^{171}Yb atoms is the $6s^2\ ^1S_0 - 6s6p\ ^1P_1$ at 399 nm, with a decay rate of $\gamma = 182.21 \times 10^6\text{ s}^{-1}$. To perform the numerical simulations we make use of the Monte Carlo Wave Function formalism that allows for the description of a single two-level atom interacting with a laser beam as a coherent and continuous Rabi-type evolution interrupted, in a random way, by spontaneous emission processes. Within this formalism we obtain that it is possible to cool ^{171}Yb atoms with initial velocities of about 300 cm/s down to a few cm/s in about 12 cm.

Keywords: cold atoms, Zeeman slower, Doppler cooling, Ytterbium, Monte Carlo Wave Function

1. Introduction

Ultracold atoms are a very useful physical platform for many areas of research, such as high-precision measurements, quantum information processing, cold chemistry, or atomic clocks [1, 2, 3]. Therefore, the production of a sufficiently high flux of ultracold atoms by optical and/or magnetic means is of utmost importance for their use in both fundamental and applied physics.

Nowadays, cooling technologies are able to reduce the kinetic energy of atoms so that their associated temperatures reach the μK regime. At this point, the quantum-mechanical properties of the atoms become dominant and determine their dynamics. To reach these temperatures, it is necessary to combine several techniques. Typically, one starts from an oven, which contains the atomic gas at room or higher temperature. From the oven, the atoms are extracted in the form of a collimated atomic beam whose longitudinal temperature is determined by the oven temperature. The atomic beam is then propagated through a Zeeman slower [4, 5] where the atoms are pre-cooled so that they can be captured and further cooled in a Magnetic Optical Trap (MOT) to reach the working temperature.

In the Zeeman slower the atoms absorb resonant photons from a counter-propagating laser beam. The momentum exchange with the photons is the key element that reduces the longitudinal velocity and temperature of the atomic beam. The main challenge is to maintain the resonance between the two relevant levels of the atom to be cooled and the laser beam

throughout the Zeeman slower. For this purpose, two different techniques are used. Firstly, the Doppler effect is used in such a way that the atoms (counter-propagating with respect to the beam) “see” a frequency higher than the nominal frequency of the laser[2]. Secondly, the position-dependent magnetic field of the Zeeman slower produces a position-dependent Stark shift of the atomic levels. In the Zeeman slower both techniques are combined to make the interaction between atoms and light resonant at any point in space, regardless of the speed of the atoms.

In this master thesis we will describe, simulate and discuss the Doppler cooling produced by a Zeeman slower using, in particular, a Monte Carlo analysis to describe the light-matter interaction. In Section 2, we will present the theoretical background. In §2.1 we will describe the basics of laser cooling by radiation pressure. In §2.2 we will explain what is a Zeeman slower and introduce its main features and most important parameters. In §2.3 we will analyze the atomic structure of a particular atom, the ^{171}Yb , and the requirements for cooling it [6]. We will explain, in §2.4, the Monte Carlo Wave Function formalism [7] that will allow us to account for the interaction of an individual atom with the counter-propagating laser beam. In Section 3, we will present numerical simulations of the Zeeman slower operation to cool ^{171}Yb atoms using the transition $6s^2\ ^1S_0 - 6s6p\ ^1P_1$. Finally, in the conclusions we will sum up the master thesis work and discuss the results obtained with the numerical simulations comparing them with those published in the literature.

2. Theoretical background

2.1. Laser cooling

In its simplest scheme, the cooling of an atom by a laser can be easily understood from the momentum conservation laws in the photon absorption process [2]. This process is shown in Figure 1. A two-level atom moving initially at velocity v_1 in the positive direction of the z-axis absorbs a photon propagating in the opposite direction. As a consequence the linear momentum of the atom is reduced by $\hbar k$ where k is the photon wavenumber. However, the atom is now excited. By spontaneous emission, the atom emits a photon in a random direction varying this time its linear momentum in the z-axis by $\cos(\theta)\hbar k$ with θ a random angle between 0 and 2π . After a large number N of absorption and spontaneous emission processes, the linear momentum of the atom will have been reduced by $N\hbar k$ since, on average, the spontaneous emission will not have contributed to the variation of its momentum. However, it is the spontaneous emission that limits the minimum velocity the atom can reach and, consequently, the temperature at which the atom can be cooled.

On the other hand, to maximize the photon absorption rate, the interaction must be resonant. Assume that the frequency of the atomic transition is ω_0 and that the frequency of the counter-propagating laser is ω_L . If we define the nominal detuning $\Delta_0 = \omega_L - \omega_0$, the detuning for an atom moving at a velocity v in the z-axis will be: $\Delta(v) = \Delta_0 + kv$ where the product kv is the Doppler shift. As a consequence, taking into account the Doppler effect we can design the interaction with the laser so that it becomes resonant for a particular atomic velocity but as this velocity decreases the absorption will no longer be resonant. The trick to keep the interaction resonant for any velocity is to use a Zeeman slower as explained in the next subsection.

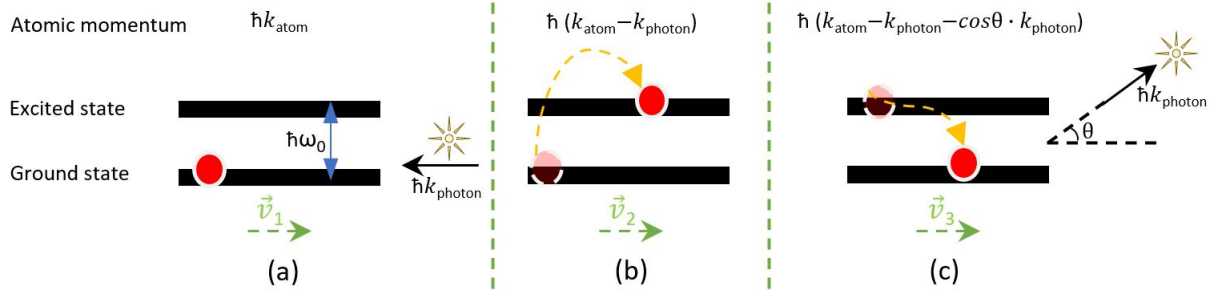


Figure 1: (a) Laser cooling of a two-level atom interacting with a resonant laser field in terms of linear momentum exchange. The absorption process (b) reduces the linear momentum of the atom and (c) the spontaneous emission produces an additional, random variation of its momentum, which is reduced to zero when integrated for many interactions.

2.2. Standard Zeeman slower

The Zeeman apparatus is basically composed of a cylinder that produces a space-dependent magnetic field inside it through the use of a solenoid coil. As can be seen in Figure 2a, the atomic beam coming from the oven propagates along the Zeeman slower interacting with the Doppler cooling laser beam. The magnetic field of the Zeeman slower, see Figure 2b, is designed so that the Doppler effect and the Stark shift in the atomic levels produced by the magnetic fields makes the interaction resonant throughout the Zeeman slower.

Now, we will review the basics of the standard Zeeman slower model. We will base the discussion on Figure 3 [4]. Along the Zeeman slower there are two frequency shifts: the Zeeman-shifted transition frequency $\omega_0 + \mu_{\text{eff}}B(z)/\hbar$, with μ_{eff} the effective magnetic moment, and the Doppler shift laser frequency $\omega_L + kv(z)$. These both frequencies shifts define the effective detuning as:

$$\Delta(z, v) = [\omega_L + kv(z)] - [\omega_0 + \mu_{\text{eff}}B(z)/\hbar] = \Delta_0 + kv(z) - \mu_{\text{eff}}B(z)/\hbar. \quad (1)$$

An ideal Zeeman slower achieves a resonance condition $\Delta(z, v) = 0$, regardless of atom's velocity. To this aim the magnetic field in terms of the atom's velocity should be:

$$B(z) = \frac{\hbar}{\mu_{\text{eff}}}(\Delta_0 + kv(z)). \quad (2)$$

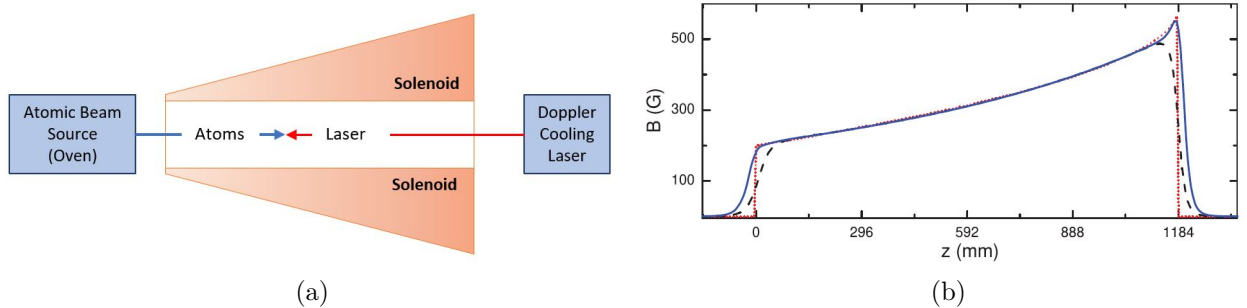


Figure 2: (a) Sketch of a Zeeman slower. Atoms reduce their velocity along the Zeeman slower due to the exchange of momentum with the counter-propagating laser beam. The role of the solenoid in the Zeeman slower is to create a spatial-dependent magnetic field that allows the atomic transition frequency to be on resonance with the Doppler-shifted laser beam frequency at any position in the slower, regardless of the atom's velocity. (b) Example of the magnetic field $B(G)$ (blue solid line) along the axis of a Zeeman slower. For details see [5].

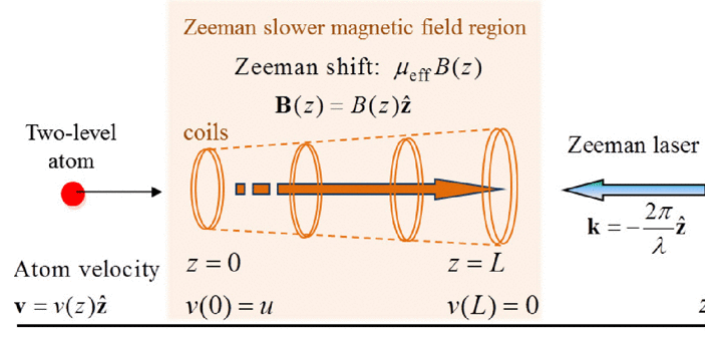


Figure 3: Basic model of the operation of a standard Zeeman slower [4]. A two-level atom of mass m propagates along the Zeeman magnetic field region, having initial velocity $\vec{v}(z) = u\hat{z}$. Its atomic transition is ω_0 plus the Zeeman shift to compensate for the decreasing of the Doppler shift as the atom absorbs photons and reduces its velocity. The counter-propagating laser with angular frequency ω_L and wavevector $\vec{k} = -k\hat{z}$ decelerates the atom by momentum exchange.

As discussed in text books [2], laser-cooling by radiation pressure for a two-level atom gives the following atom's deceleration due to the absorption of photons of the laser beam:

$$a = \frac{dv}{dt} = -\frac{1}{m} \frac{s}{1 + s + 4\Delta^2/\gamma^2} \frac{\hbar k \gamma}{2}, \quad (3)$$

where γ is the transition decay rate by spontaneous emission and $s = I/I_{\text{sat}} = 2\Omega^2/\gamma^2$ represents the laser intensity in units of the saturation intensity of the transition. $\Omega = \vec{\mu}_0 \cdot \vec{E}_0/\hbar$ is the so-called Rabi frequency with μ_0 the electric dipole moment and E_0 the electric amplitude of the laser field. In Figure 4, we plot the deceleration computed from expression (3) for the $6s^2\ ^1S_0 - 6s6p\ ^1P_1$ transition at 399 nm of a ^{171}Yb atom whose decay rate is $\gamma = 182.21 \times 10^6 \text{ s}^{-1}$. In Figure 4a, we can easily observe that for $\Delta = 0$ and Ω larger than $\sim 1000 \times 10^6 \text{ rad/s}$ saturation occurs. In Figure 4b we have fixed the Rabi frequency at $\Omega = 183.49 \times 10^6 \text{ rad/s}$ and explore how the deceleration decays as the detuning increases.

If we are able to adjust the magnetic field following Eq. (2), then $\Delta(z, v) = 0$, and Eq. (3)

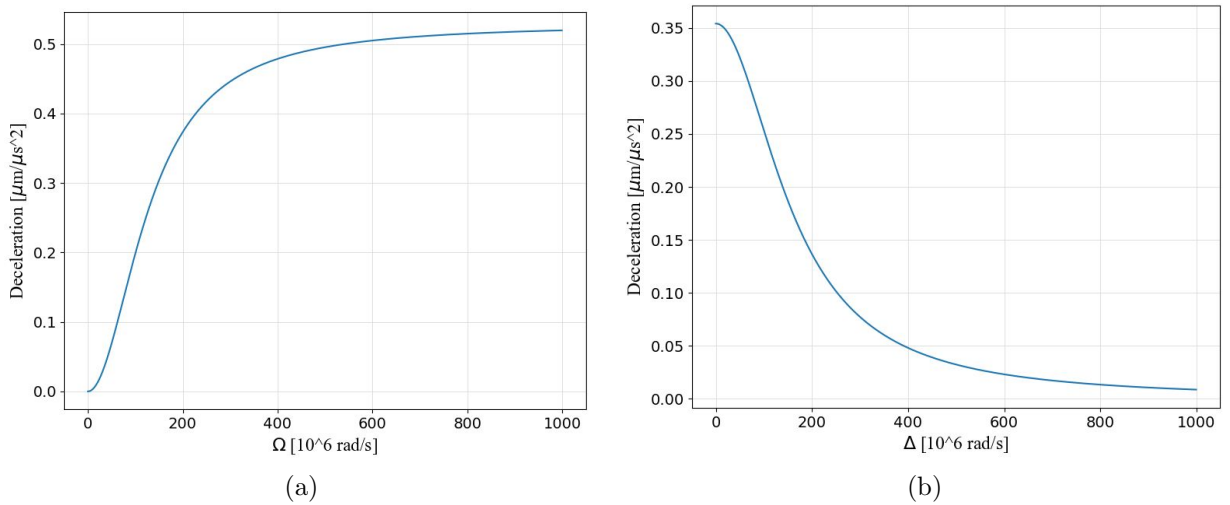


Figure 4: (a) Deceleration as a function of the Rabi frequency according to expression (3) for $\Delta = 0$. (b) Deceleration as a function of the detuning for $\Omega = 183.49 \times 10^6 \text{ rad/s}$. The rest of parameter values are $m = 2.84 \times 10^{-25} \text{ kg}$ and $\gamma = 182.21 \times 10^6 \text{ s}^{-1}$ corresponding to the mass of the ^{171}Yb atom and the decay rate of its transition $6s^2\ ^1S_0 - 6s6p\ ^1P_1$.

simplifies to:

$$\frac{dv}{dt} = -\eta \frac{\hbar k \gamma}{2m} = -\eta a_{\max}, \quad (4)$$

where $\eta = s/(1+s)$ and $a_{\max} = \hbar k \gamma / 2m$, which is obtained when $I \rightarrow \infty$ and can be understood as the maximum possible magnitude of the deceleration for a fully saturated transition. The velocity profile is obtained from Eq. (4) multiplying by $\frac{dz}{dz}$ and integrating:

$$\frac{dz}{dt} \frac{dv}{dz} = v \frac{dv}{dz} = -\eta a_{\max}, \quad \int_{v_0=u}^v v \cdot dv = -\eta a_{\max} \int_{z_0=0}^{z=L} dz. \quad (5)$$

Finally:

$$v(z) = \sqrt{u^2 - 2\eta a_{\max} z}. \quad (6)$$

If $v(z) = 0$, the atoms stop at $L = u^2/(2\eta a_{\max})$. By introducing this expression into (6), we rewrite $v(z)$ as:

$$v(z) = u \sqrt{1 - \frac{z}{L}}. \quad (7)$$

Introducing this last expression in (2) we obtain a much clearer expression for the magnetic field of the Zeeman slower:

$$B(z) = B_L \sqrt{1 - \frac{z}{L}} + B_0, \quad (8)$$

where $B_L = \hbar k u / \mu_{\text{eff}}$ and $B_0 = \hbar \Delta_0 / \mu_{\text{eff}}$. The first term in the r.h.s. of (8) takes into account the spatial dependence of $B(z)$, while the second one is a constant proportional to the nominal laser detuning Δ_0 . Clearly, the magnetic field of the Zeeman slower is designed to slow-down atoms with a particular initial velocity u and a with particular nominal detuning Δ_0 .

2.3. Considerations for ^{171}Yb

^{171}Yb is a stable isotope of ytterbium and is a strong candidate for many applications ranging from quantum computation to high-precision measurements such as for optical lattice clocks [8, 9, 6]. This is due to the fact that it has experimentally accessible optical transitions, which not only allow ^{171}Yb to be laser-cooled and trapped, but also to reach Bose-Einstein condensation [9]. The atomic level structure of ^{171}Yb is shown in Figure 5a [8]. Two possible transitions one at 399 nm and another at 556 nm can be used for Doppler laser cooling. However, being the decay rate of the $6s^2\ ^1S_0 - 6s6p\ ^1P_1$ at 399 nm much larger than that of the $6s^2\ ^1S_0 - 6s6p\ ^3P_1$ at 556 nm, the first is much more appropriate for laser cooling in the Zeeman slower. The decay rate of this transition is $\gamma = 182.21 \times 10^6\ \text{s}^{-1}$. Regarding the Doppler cooling procedure, the standard protocol is to use a frequency-doubled Titanium:Sapphire laser locked to the atomic resonance at 399 nm.

^{171}Yb is solid at room temperature so it needs to be heated in an oven at high temperatures to coexist with a significant vapor fraction. Typically, the temperature is raised in the range of 400 to 600 degrees Celsius. The higher the oven temperature, the higher the density of Ytterbium vapor will be generated, but the higher the average velocity of the atoms. Once the ^{171}Yb atoms are extracted from the oven in the form of an atomic beam, the Maxwell-Boltzmann velocity distribution is given by:

$$f(v, T) = 4\pi v^2 \left(\frac{m}{2\pi k_B T} \right)^{3/2} e^{-\frac{mv^2}{2k_B T}}, \quad (9)$$

where $f(v, T)dv$ gives the probability for an atom to have a velocity between v and $v + dv$ at a temperature T , m is the mass of the atom and k_B is Boltzmann's constant. Figure 5b shows the velocity distribution for an atomic beam of ^{171}Yb atoms at $T = 706\ \text{K}$.

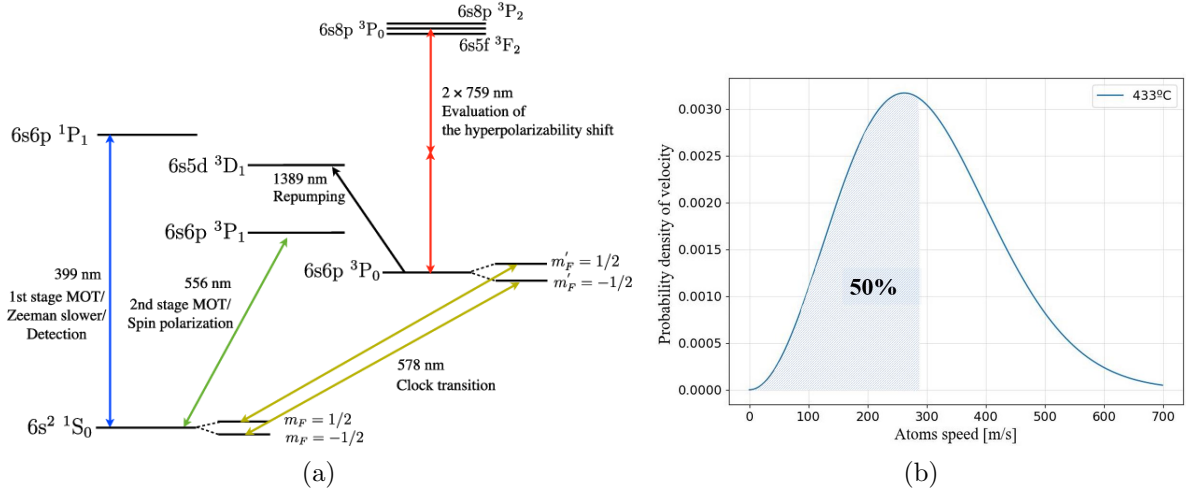


Figure 5: (a) Energy diagram of ^{171}Yb atomic levels. We will use $6s^2\ ^1S_0 - 6s6p\ ^1P_1$ as the transition for Doppler cooling in the Zeeman slower. (b) Maxwell-Boltzmann atomic velocity distribution for an atomic beam of ^{171}Yb atoms at $T = 706\text{ K}$. Note that the distribution is not symmetric. It has a peak at 257 m/s but one needs to integrate between 0 and 285 m/s to select the 50% of the atoms of the atomic beam.

2.4. Monte Carlo Wave Function formalism

In the Monte Carlo Wave Function (MCWF) formalism [7], the dynamics of a two-level atom, with ground state $|g\rangle$ and excited state $|e\rangle$, interacting with a continuous wave laser field with Rabi frequency Ω and detuning Δ is governed by the following Hamiltonian:

$$H = -\hbar(\Delta + i\gamma)S^+S^- + \hbar\left(\frac{\Omega}{2}\right)(S^+S^- + S^-S^+), \quad (10)$$

where S^+ and S^- are raising and lowering operators defined as $S^+ = |e\rangle\langle g|$, and $S^- = |g\rangle\langle e|$, respectively. γ is the spontaneous emission decay rate from $|e\rangle$ to $|g\rangle$.

At an initial time t , the system can be represented as $|\psi(t)\rangle = |\phi(t)\rangle \otimes |0\rangle$ where $|\phi(t)\rangle$ accounts for the atomic state, $|0\rangle$ represents the ground state containing zero photons of the electromagnetic field in the spontaneous emission modes, and $|\psi(t)\rangle$ corresponds to the state of the total system. At time $t + dt$ there are two possible situations, depending on whether a spontaneous emission has taken place or not. We define $dp = \gamma p_e(t)dt$, with p_e the excited state population, as the probability for a spontaneous emission in a time interval dt . At time $t + dt$ we generate a random number $\varepsilon \in (0, 1)$ and two possibilities can take place

$$\begin{aligned} \text{If } dp < \varepsilon < 1 &\longrightarrow |\psi(t + dt)\rangle = \mu(a'_g|g\rangle + a'_e|e\rangle) \otimes |0\rangle, \\ \text{If } 0 < \varepsilon < dp &\longrightarrow |\psi(t + dt)\rangle = |g\rangle \otimes |1\rangle \rightarrow |g\rangle \otimes |0\rangle, \end{aligned} \quad (11)$$

where a'_g and a'_e are the probability amplitudes for the atom to be in states $|g\rangle$ and $|e\rangle$ at time $t + dt$, respectively, given by the integration of the Schrödinger equation with Hamiltonian (10). $\mu = 1/\sqrt{1 - dp}$ is the normalisation factor. In (11) we assume that once the atom emits a photon this is automatically removed from the spontaneous emission modes since it is absorbed by a detector. It is important to highlight that it has been demonstrated that averaging over many realizations of the MCWF approach exactly reproduces the results that would be obtained from the density matrix formalism [7]. Finally, each time that a spontaneous emission occurs it means that the atom has absorbed a photon from the laser and emitted another one by spontaneous emission. In the absorption of a laser photon the momentum of the atom along the Zeeman slower axis is reduced by $\hbar k$ where k is the laser wave number. However, as

the spontaneously emitted photon is emitted in a random direction the momentum exchange between the atom and the spontaneously emitted photon will be $\cos(\pi\varepsilon')\hbar k$ where ε' is another random number between 0 and 1.

3. Numerical results

In this section we will present the numerical results obtained from the simulation of the operation of the Zeeman slower. As explain before, we consider the $6s^2\ ^1S_0 - 6s6p\ ^1P_1$ transition of ^{171}Yb at 399 nm with a decay rate of $\gamma = 182.21 \times 10^6\text{ s}^{-1}$. We choose a Rabi frequency of $\Omega = 183.49 \times 10^6\text{ rad/s}$ such that, assuming on-resonance interaction, the predicted deceleration becomes $a = 0.354\ \mu\text{m}/\mu\text{s}^2$, see Figure 4b. Note that with a larger Rabi frequency we could further increase the deceleration rate up to about $a = 0.528\ \mu\text{m}/\mu\text{s}^2$, see Figure 4a. To start with, we take a single ^{171}Yb atom with initial velocity $u = 285\text{ m/s}$.

3.1. Cooling of a single atom without the Zeeman slower

We will first check the effect of Doppler cooling when there is no Zeeman Slower and, therefore, there is no Zeeman shift of the atomic levels. In this scenario, we take the nominal detuning of the laser such that the effective detuning that takes into account atom's initial velocity u is zero. Therefore, the interaction is on resonance at the beginning but becomes out of resonance as soon as the atom reduces its speed. This is perfectly clear in Figure 6a, where full Rabi oscillations (a signature of on-resonance interaction) are present at the beginning but very quickly become incomplete as the atom reduces its velocity and becomes out of resonance. As a consequence, see Figure 6b, the atom initially reduces its velocity but, afterwards, this reduction in velocity becomes very small.

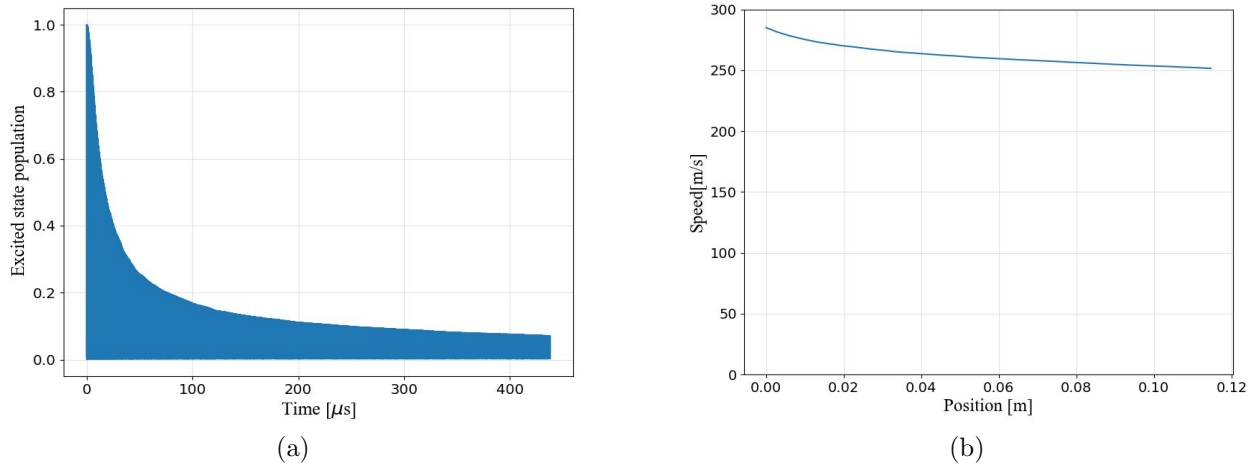


Figure 6: (a) Time evolution of the population (normalized to 1) of the excited state $6s6p\ ^1P_1$ of ^{171}Yb . (b) Atom's velocity as a function of the position. Parameter values: $\gamma = 182.21 \times 10^6\text{ s}^{-1}$, $\Omega = 183.49 \times 10^6\text{ rad/s}$, and $u = 285\text{ m/s}$.

3.2. Cooling of a single atom with the Zeeman slower

Now we assume that the Zeeman slower creates the position-dependent magnetic field given by Equation (9). In this case, we expect that the interaction will be resonant all along the Zeeman slower. In Figure 7a we observe almost full Rabi oscillations between states $6s^2\ ^1S_0$ and $6s6p\ ^1P_1$ during $\sim 800\ \mu\text{s}$. At this particular time, the ^{171}Yb atom is stopped. The fluctuations

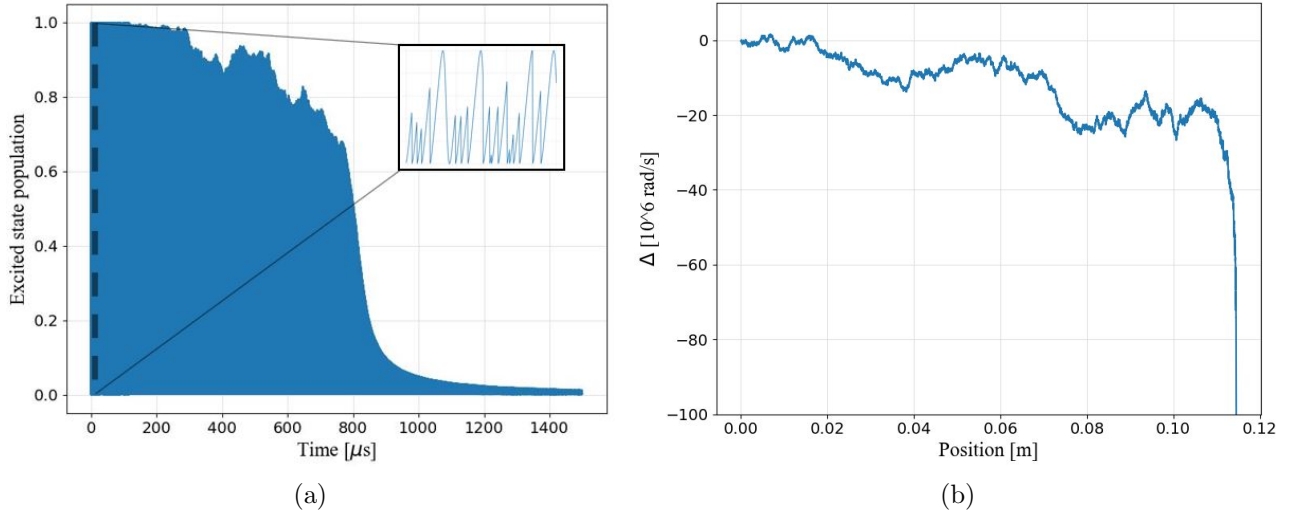


Figure 7: (a) Time evolution of the population (normalized to 1) of the excited state $6s6p^1P_1$ of ^{171}Yb . (b) Atom's detuning as a function of the position. Parameter values: $\gamma = 182.21 \times 10^6 \text{ s}^{-1}$, $\Omega = 183.49 \times 10^6 \text{ rad/s}$, and $u = 285 \text{ m/s}$.

in the maximum population of the Rabi oscillations are due to the stochastic nature of the interactions, as seen in Figure 7b. In fact, the detuning is noisy due to the random direction of the spontaneously emitted photons. However, the detuning is close to zero till time $\sim 800 \mu\text{s}$ corresponding to a propagated distance of $\sim 11.5 \text{ cm}$.

Figures 8a and 8b show atom's velocity as a function of time and position, respectively. It is clear from Figure 8a the constant deceleration of atom's trajectory. In fact the slope of this curve gives a deceleration of $0.35 \mu\text{m}/\mu\text{s}^2$, which almost matches the expected one of $0.354 \mu\text{m}/\mu\text{s}^2$. Figure 8b shows atom's velocity as a function of the position. Clearly, the atom stops at $\sim 11.5 \text{ cm}$ and even takes negative velocities later on since still absorbs counter-propagating photons.

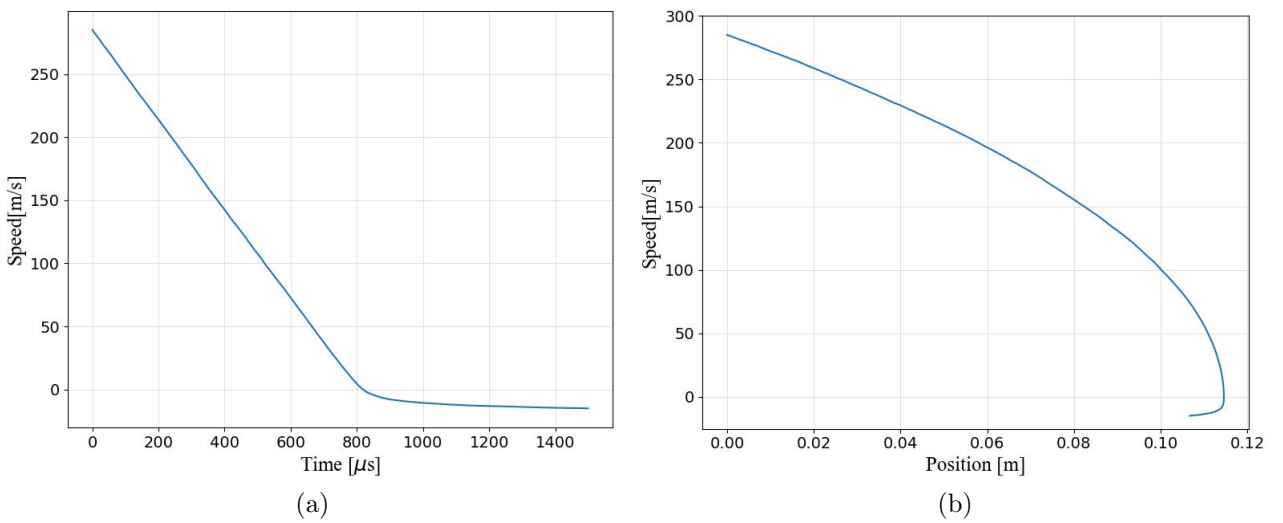


Figure 8: Atom's velocity as a function of (a) time and (b) position. Parameter values as in Figure 7.

3.3. Cooling of an atomic beam with a Zeeman slower designed for $u = 300$ m/s

In the two previous subsections we have considered an atom with a specific input velocity. In this subsection we will consider an atomic beam of ^{171}Yb that possesses a temperature-dependent velocity distribution, see Figure 5b. We assume that the Zeeman slower is designed to cool atoms propagating at an input velocity of $u = 300$ m/s and we are going to see what happens to atoms that are sent at input velocities lower or higher than this reference velocity.

Figure 9a shows, for different input velocities, atom's velocity as a function of the position in the Zeeman slower. As the Zeeman slower is designed for $u = 300$ m/s, atoms with this input velocity are resonant with the laser photons all along the Zeeman slower so the deceleration is constant till these atoms are stopped. Atoms with input velocities larger than 300 m/s are far out of resonance with the laser as a consequence of the Doppler effect. In these cases, the Zeeman effect is not able to compensate the Doppler effect at any time and there is practically no photon absorption. As a consequence, the velocity of these atoms does not vary in the Zeeman slower. The situation is completely different for atoms with initial velocities of less than 300 m/s, see, for instance, the case of $u = 175$ m/s of Figures 9a and 9b. In this case, the interaction is non-resonant at the beginning of the Zeeman slower but at a particular point of the Zeeman slower the compensation of the Zeeman effect and the Doppler effect is perfect such that the interaction becomes resonant. From this point on, the interaction is always resonant until the atom stops. This is the explanation why all the curves with initial velocities less than 300 m/s end up fitting each other.

As the integrated probability distribution between 0 and 300 m/s of the ^{171}Yb atomic beam gives slightly more than half of the total beam population at $T = 706\text{K}$, the results shown in Figure 9a indicate that a Zeeman slower with about 12 cm is able to cool about 50% of the atoms of the ^{171}Yb beam such that they reach output velocities of a few cm/s.

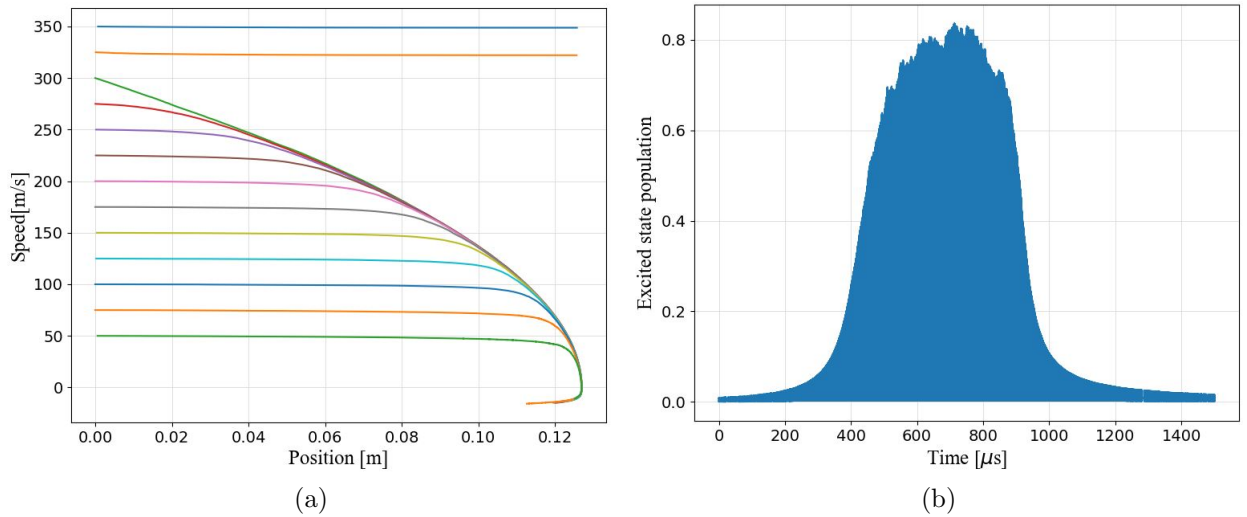


Figure 9: (a) Atom's velocity as a function of the position. The Zeeman slower is designed for an atom's input velocity of $u = 300$ m/s but it perfectly works for all atoms moving with input velocities smaller than the 300 m/s. In (b) we show the time evolution of the population of the excited state $6s6p^1P_1$ of ^{171}Yb for an input velocity of $u = 175$ m/s.

4. Conclusions

A major part of modern technologies are based on microelectronics and classical communications and computing. The next big technological step will be to expand the use of photonics and incorporate quantum communications and computing. In particular, the advancement of quantum technologies will depend on the ability to precisely control and manipulate quantum physical systems. Among the possible physical platforms for implementing quantum technologies are ultracold atoms captured and manipulated with laser light. In this context, laser cooling is a fundamental tool.

In this master work we have discussed the cooling of ^{171}Yb atoms in a Zeeman slower. We have studied how the combination of the Doppler effect and the Stark effect in the Zeeman slower allows to maintain on-resonance absorption along the slower and, consequently, to cool ^{171}Yb atoms by means of the linear momentum exchange between the atoms and the light. To describe the interaction between light and matter we have used the Monte Carlo Wave Function formalism, which has allowed us to associate a momentum exchange to the absorption and spontaneous emission processes and, consequently, to study the individual trajectory of a single atom in the Zeeman slower.

In particular, we have considered the $6s^2\ ^1\text{S}_0 - 6s6p\ ^1\text{P}_1$ transition of ^{171}Yb at 399 nm for Doppler cooling and assumed a magnetic field in the Zeeman slower capable of maintaining the on-resonance condition with the laser for any atom velocity. By Monte Carlo simulations we have determined that it is possible to cool ^{171}Yb atoms with initial velocities equal to or less than 300 m/s at distances of the order of 12 cm. Note that in other published works with ^{171}Yb [4], a Zeeman slower of about 70 cm was used to cool atoms with initial velocities similar to those of our work, while in the case of ^{87}Rb , Zeeman slowers of about 1 m in length are commonly used to cool atoms with input velocities of ~ 400 m/s [5].

References

- [1] M. Lewenstein, A. Sanpera, and V. Ahufinger. “Ultracold Atoms in Optical Lattices”. In: *Oxford University Press First Edition* (2012).
- [2] C. S. Adams and E. Riis. “Laser cooling and trapping of neutral atoms”. In: *Progress in Quantum Electronics* 21.1 (1997), pp. 1–79.
- [3] P. J. Ungar et al. “Optical molasses and multilevel atoms: theory”. In: *J. Opt. Soc. Am. B* 6 (Nov. 1989), pp. 2058–2071.
- [4] S. A. Hopkins et al. “A versatile dual-species Zeeman slower for caesium and ytterbium”. In: *Review of Scientific Instruments* 87 (2016), p. 043109.
- [5] P. Cheiney et al. “A Zeeman slower design with permanent magnets in a Halbach configuration”. In: *Review of Scientific Instruments* 82 (2011), p. 063115.
- [6] H. S. Margolis. “Metrology: Lattice clocks embrace ytterbium”. In: *Nature Photonics* 3 (2009), pp. 557–558.
- [7] J. Dalibard, Y. Castin, and K. Mølmer. “Wave-function approach to dissipative processes in quantum optics”. In: *Phys. Rev. Lett.* 68 (1992), pp. 580–583.
- [8] T. Kobayashi et al. “Uncertainty Evaluation of an ^{171}Yb Optical Lattice Clock at NMIJ”. In: *IEEE Transactions on Ultrasonics, Ferroelectrics, and Frequency Control* 65 (2018), pp. 2449–2458.
- [9] Y. Takasu et al. “Spin-Singlet Bose-Einstein Condensation of Two-Electron Atoms”. In: *Phys. Rev. Lett.* 91 (2003), p. 040404.